



Yu, Q., Pichugin, D., Cruz, M., Guerin, G., Manners, I., & Winnik, M. A. (2018). NMR Study of the Dissolution of Core-Crystalline Micelles. *Macromolecules*, 51(9), 3279-3289.  
<https://doi.org/10.1021/acs.macromol.8b00098>

Peer reviewed version

License (if available):  
Unspecified

Link to published version (if available):  
[10.1021/acs.macromol.8b00098](https://doi.org/10.1021/acs.macromol.8b00098)

[Link to publication record in Explore Bristol Research](#)  
PDF-document

This is the author accepted manuscript (AAM). The final published version (version of record) is available online via ACS at <https://pubs.acs.org/doi/10.1021/acs.macromol.8b00098> . Please refer to any applicable terms of use of the publisher.

## University of Bristol - Explore Bristol Research

### General rights

This document is made available in accordance with publisher policies. Please cite only the published version using the reference above. Full terms of use are available:  
<http://www.bristol.ac.uk/red/research-policy/pure/user-guides/ebr-terms/>

# NMR Study of the Dissolution of Core-Crystalline Micelles

Qing Yu<sup>1</sup>, Dmitry Pichugin<sup>1</sup>, Menandro Cruz<sup>1</sup>, Ian Manners<sup>2</sup>, and Mitchell A. Winnik<sup>1\*</sup>

<sup>1</sup> Department of Chemistry, University of Toronto, 80 St. George Street, Toronto, ON, M5S 1H6

<sup>2</sup> School of Chemistry, University of Bristol, Bristol, UK, BS8 1TS

## ABSTRACT

The core-crystalline micelles formed by block copolymer (BCP) poly(ferrocenyldimethylsilane)-*block*-poly(isoprene) (PFS-*b*-PI) underwent self-seeding in solution when heated above

dissolution temperature. Variable temperature (VT) proton ( $^1\text{H}$ ) NMR and diffusion-ordered pulsed-gradient spin-echo (DOSY) NMR were used to monitor the behavior of micelles that dissolved as a function of temperature. We examined a sample of micelle fragments of PFS<sub>65</sub>-*b*-PI<sub>637</sub> characterized by  $L_n = 39$  nm,  $L_w/L_n = 1.13$ . The PI corona had high mobility and gave a  $^1\text{H}$  NMR signal in both micellar and unimers forms. Whereas the PFS component could only be detected for the dissolved unimers. We found from  $^1\text{H}$  NMR that all the BCP molecules were incorporated into the micelles at temperatures up to and including 50 °C. Both PFS and PI resonances could be detected between 70 and 100 °C, and the integration ratio of the PFS-to-PI peaks increased with temperature. The DOSY NMR measured the self-diffusion coefficients ( $D_s$ ) for the micelle fragments and unimers at these temperatures. The hydrodynamic radii ( $R_h$ ) for these species were calculated from  $D_s$  using Stokes-Einstein equation. The PFS signals gave  $R_h$  values in the range of 5 to 6 nm at temperatures between 80 to 100 °C, consistent with unimer diffusion. PI signals were fitted into a single exponential decay at 25 °C with  $R_h = 38$  nm characteristic of the micelle fragments, and at 90, 95, and 100°C with  $R_h \approx 6$  nm, corresponding to unimer. At intermediate temperatures (70 to 85 °C), PI signals were fitted to a sum of two exponential terms, consistent with a fast diffusing species and a slow diffusing species. Interestingly we noticed that the size of the micelle fragments at elevated temperatures (80, 85 °C) was sensitive to sample history, with smaller fragments obtained for samples heated quickly to the measurement temperature while samples subjected to prolonged annealing showed much smaller reduction in size.

## INTRODUCTION

The self-assembly of block copolymers (BCPs) in solution has been a topic of broad interest for many years.<sup>1</sup> In selective solvents, these BCPs form core-shell structures with an insoluble

core surrounded by a solvent swollen corona, in which the shapes of the colloidal objects depend upon the composition of the BCP and the nature of the solvent. In self-assembly, the entropy of the single chain is sacrificed in order to avoid a larger enthalpy penalty resulting from energetically unfavorable interactions between the core block and the solvent, lowering the total free energy of the system ( $\Delta G < 0$ ). There are three main contributions to the free energy of the system that determine the shapes of the objects formed: the degree of stretching of the core-forming blocks, the interfacial tension between the micelle core and the solvent outside the core, and the repulsive interactions among corona-forming chains.<sup>2</sup> The most common morphologies are spherical and cylindrical micelles as well as bilayer vesicles.

Among these morphologies, elongated structures (cylindrical “worm-like” and rod-like micelles) are of increasing importance as they have promising applications in nanotechnology and medicine.<sup>3</sup> For example, Bates and coworkers<sup>4</sup> showed that worm-like micelles of poly(ethylene oxide)-poly(ethylene-alt-propylene) (PEO-PEP) serve as effective impact modifiers to reduce the brittleness of epoxy resins. Discher and co-workers<sup>5</sup> reported the use of elongated “filomicelles” formed from poly(ethylene glycol) (PEG)-based BCPs as drug carriers in animal studies. These micelles had much longer blood residence times than corresponding spherical micelles. In coil-coil block polymer system, which form micelles with an amorphous core, cylindrical micelles are normally formed for only a narrow range of compositions in which the height of the corona chains is smaller than the radius of the insoluble polymer core.<sup>1</sup>

In contrast, crystalline-coil BCPs, where crystallization of the core-forming block plays an important role in self-assembly, elongated fiber-like micelles are much more common, particularly when the corona block is much longer than the core-forming block. A cylindrical morphology can be achieved with a wide range of block ratios and compositions, but particularly in the case of long-corona forming blocks.<sup>6</sup> Examples of the crystallizable core-forming block include poly(ferrocenyldimethylsilane) (PFS),<sup>7</sup> polycaprolactone,<sup>8, 9</sup> poly(L-lactic acid),<sup>10, 11</sup> polyethylene,<sup>12</sup> polyacrylonitrile,<sup>13</sup> poly(3-hexylthiophene),<sup>14, 15</sup> and poly(3-alkylselenophene).<sup>16</sup> In the case where the self-assembly process occurs because of the crystallization of the core-forming block, we refer to the process as “crystallization-driven self-assembly”, CDSA.<sup>17</sup> Under special circumstances, particularly with PFS BCPs, one can use micelle fragments as seeds to initiate the growth of elongated micelles upon addition of more BCP as a solution (of unimers) in a common good solvent like THF. Under these circumstances, the added unimers deposits

epitaxially on the ends of the growing micelles, and the micelles grow at a common rate, leading in the end to micelles with a very narrow length distribution. This initiated growth process has many features in common with the living polymerization of molecular monomers, and we refer to this process as living CDSA.

Core-crystalline rod-like PFS BCP micelles also exhibit another feature common to polymer crystals: they undergo self-seeding when a solution of the micelle fragments in a selective solvent is heated, forming longer micelles of uniform length upon cooling.<sup>18-20</sup> The process of self-seeding was first identified in the 1960s as a way of preparing uniform single crystals of common crystalline polymers such as polyethylene and poly(ethylene glycol).<sup>21</sup> In this experiment, one heats a suspension of the crystalline polymer until it appears to dissolve and the solution turns clear. Upon cooling, polymer crystals form, nucleated by the very small number of seed nuclei that survive the annealing. The size of the polymer crystals formed and their number is very sensitive to the annealing temperature. What one learns from this experiment is that polymer crystals are not uniform and are characterized by a distribution of domains of different degrees of crystal perfection. Upon annealing, the polymer in the less crystalline domains dissolves, leaving the more crystalline domains intact. At higher temperatures, only the most crystalline domains survive. The number of these crystallites decreases exponentially with increasing temperature, leading to a smaller number of larger crystals upon cooling. Since the number of crystals formed and their size is independent of the annealing time, one believes that the surviving seeds in the hot solution are at thermodynamic equilibrium. We also understand that the degree of crystallinity of a polymer sample depends on many factors such as the crystal growth rate, the age of the crystal, and its thermal history.<sup>22</sup> Thus these factors should have an important effect on the fraction of crystallites that survive heating in a solvent to a given temperature.

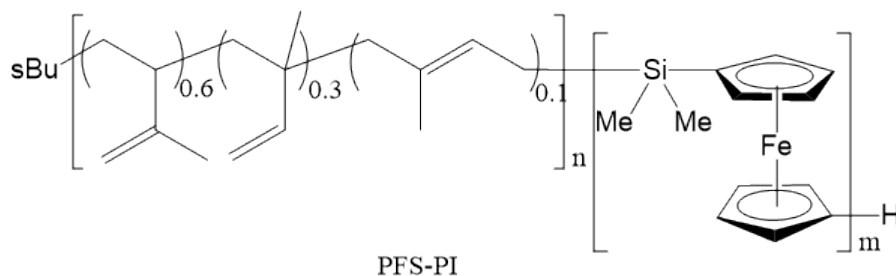
Most of our ideas about the mechanism of self-seeding are based on observations of the size of crystals obtained following a heating and cooling cycle. This model anticipates that during the heating cycle, the solution consists of a mixture of molecularly dissolved polymer (unimer) and intact seed crystallites. We are particularly interested in developing a deeper understanding of how self-seeding operates on solutions of core-crystalline BCP micelles. Here at elevated temperatures, the solution should consist of a mixture of unimer and colloidally stable micelles. We are unaware of previous experiments that attempt to monitor directly the fraction of polymer

that has dissolved for samples annealed at different temperatures. Here we explore the idea that variable temperature NMR and DOSY NMR measurements can provide important new insights into the polymer dissolution process.

Diffusion-ordered spectroscopy (DOSY) NMR is a powerful tool for the analysis of mixtures.<sup>23</sup> It is based on pulsed field gradient-spin echo (PFG-SE) NMR methodology that itself is often used to measure self-diffusion coefficients ( $D_s$ ) in a variety of different systems such as colloids and polymers.<sup>24</sup> The ability of PFG-SE NMR to analyze mixtures with overlapping resonances from different components makes it possible to study different components present in same sample individually. For example, Muller et al.<sup>25</sup> demonstrated the use of DOSY NMR to investigate polymer mixtures and molecular weight distribution. Bertin et al. performed a compositional analysis on mixtures of a polystyrene-poly(ethylene oxide) BCPs (PS-*b*-PEO) and the unreacted end-functionalized PEO homopolymer in the polymerization. In this way, they demonstrated that DOSY is an effective method to monitor the polymerization and purification procedures.<sup>26</sup> The use of DOSY to study self-assembly processes has also been reported. Johnson and co-workers<sup>27</sup> used PFG NMR to follow the self-assembly of poly(vinyl acetate)-*b*-poly(1,1-dihydroperfluorooctyl acrylate) (PVAc-*b*-PFOA) and polystyrene-*b*-poly(1,1-dihydroperfluorooctyl acrylate) (PS-*b*-PFOA) BCPs in liquid CO<sub>2</sub>. Coudane et al.<sup>28</sup> showed that the critical micelle concentration (CMC) of the amphiphilic poly(lactic acid)-*b*-poly(ethylene glycol)-*b*-poly(lactic acid) (PLA-*b*-PEG-*b*-PCL) triblock terpolymer could also be obtained using this technique. In previous studies reported by our group,<sup>29</sup> we used PFG NMR to examine the ligand exchange process in which a linear polymer, poly(2-(N,N-dimethylamino)ethyl methacrylate), displaced trioctylphosphine oxide (TOPO) from the surface of TOPO-coated CdSe quantum dots.

In this paper, we examine the behavior of PFS-*b*-PI micelles in decane subjected to self-seeding conditions. We use a combination of variable temperature <sup>1</sup>H NMR (VT-NMR) and DOSY NMR measurements to monitor micelle fragment samples of PFS<sub>65</sub>-*b*-PI<sub>637</sub>, where the subscripts refer to the number average degree of polymerization. Its structure is presented in Scheme 1. At room temperature, all of the polymer molecules are incorporated into the micelles. In <sup>1</sup>H NMR spectra, after suppression of the decane peaks, only signals from the PI corona chains can be detected, and the DOSY signal gives a  $D_s$  value consistent with the diffusion of short micelles. At 100 °C, all the polymer molecules dissolve, and signals from the both

ferrocene protons of the PFS and those of the PI protons are prominent. Here the DOSY signal gives a  $D_s$  value consistent with the diffusion of molecularly dissolved unimers. These experiments allow us to monitor directly the fraction of polymer in the micelles that has dissolved at each annealing temperature and also provide insights into changes in size of the surviving micelle fragment seeds. Over a small range of temperatures in the range of 70 to 85° C it is possible to detect simultaneously the diffusion of the micelles and unimers, but the most precise values of the fraction of polymer in the micelles that has dissolved comes from the integration of the PFS and PI signals in the  $^1\text{H}$  NMR spectra.



**Scheme 1.** The chemical structure of the BCP  $\text{PFS}_{65}\text{-}b\text{-PI}_{637}$ . The microstructure of the PI block originates from its synthesis in THF.

## EXPERIMENTAL

### *Purification of block copolymer $\text{PFS}_{65}\text{-}b\text{-PI}_{637}$*

The  $\text{PFS}_{65}\text{-}b\text{-PI}_{637}$  sample is the same polymer originally described in Ref. 30. It was originally reported to have a composition  $\text{PFS}_{53}\text{-}b\text{-PI}_{637}$ . This composition was determined in two steps. First an aliquot of the PI block was taken from the synthesis and analyzed by gel permeation chromatography. Its number average degree of polymerization ( $\text{DP}_n$ ) was determined to be 637.<sup>30</sup> The corresponding length of the PFS block was determined by comparing integration values of the PFS and PI signals in the  $^1\text{H}$  NMR. At the beginning of the experiments reported here, DOSY measurements showed the presence of a small amount of PI homopolymer. This impurity was removed by fractional precipitation. The polymer was dissolved in minimum amount of THF and sonicated briefly to promote complete dissolution. The polymer solution was then transferred into hexane in a vial and allow to stand for an hour. This solution was then diluted with more hexane, transferred into 4 7-mL vials and allowed to stand overnight. This process led to the formation of long fiber-like micelles. The resulting solution was centrifuged

three times at 20000 rpm for 20 min, followed by removal of the supernatant. Here, comparison of the  $^1\text{H}$  NMR integration values of the PFS and PI signals led to a composition of PFS<sub>65</sub>-*b*-PI<sub>637</sub> for the purified polymer.

### ***Preparation of PFS<sub>65</sub>-*b*-PI<sub>637</sub> micelle seed fragments***

PFS<sub>65</sub>-*b*-PI<sub>637</sub> (30 mg) was added to decane (5 mL) and then heated at 100 °C for 15 min to dissolve the sample. Upon slow cooling to room temperature (23 °C), long micelles (> 1 μm) of uniform width were obtained. This micelle solution was then subjected to sonication in a 60 watt sonication bath for 30 min (3×10 min intervals) at room temperature. Short micelle fragments were obtained with number and weight average lengths, respectively, of  $L_n = 39$  nm and  $L_w = 44$  nm.

### ***NMR Spectroscopy Experiments***

All NMR experiments were performed on an Agilent DD2 600 spectrometer. The concentrations of both the PFS<sub>65</sub>-*b*-PI<sub>637</sub> unimer solution in benzene-*d*<sub>6</sub> and micelle fragment solutions in decane were 6 mg/mL. All experiments were run with a capillary insert containing DMSO-*d*<sub>6</sub> as a deuterium lock.

**Variable temperature (VT)  $^1\text{H}$  NMR.** Proton NMR spectra of PFS<sub>65</sub>-*b*-PI<sub>637</sub> micelle fragment solutions in decane were obtained at various temperatures that ranged from 25 to 100 °C. Two spectra were taken at each temperature examined: the first was recorded when the sample just reached the desired temperature, and the second one was recorded after equilibrating for 15 min.

**DOSY NMR.** DOSY experiments employed the Pulse Field Gradient Spin Echo NMR technique using a pulse sequence [Pulse Field Gradient Double STimulated Echo (Dpfgdste)] proposed by Jerschow and Muller<sup>25</sup> to compensate for complications caused by convection in liquid samples at elevated temperatures. This pulse sequence is presented in Figure S1, Supporting Information (SI). The diffusion coefficient of a single diffusing species<sup>31</sup> in a sample can be calculated from the expression

$$I = I_0 \exp(-2\tau_2/T_2) \exp(-\tau_1/T_1) \exp[-(\gamma g \delta)^2(\Delta - \delta/3)D_s] \quad (1)$$

where  $D_s$  is the self-diffusion coefficient,  $T_1$  and  $T_2$  are the longitudinal and transverse relaxation times, respectively.  $\delta$  is the diffusion gradient length,  $\gamma$  is the particular magnetogyric ratio,  $g$  is the magnitude of the gradient pulse, and  $\Delta = \tau_2 + \tau_1$  is the diffusion delay time. A value of  $\tau_2 = 5$



ms was used in all measurements, and the value of  $\tau_1$  changed accordingly with diffusion delay.

For a mixture that consists of two independently diffusing species with overlapping resonances, such as the PFS-PI unimers and PFS-PI micelles in high temperature decane solution, the diffusion decay is the sum of two exponential terms

$$I/I_0 = \sum f_i \exp(-2\tau_2/T_{2i}) \exp(-\tau_1/T_{1i}) \exp[-(\gamma g \delta)^2 (\Delta - \delta/3) D_i] \quad (2)$$

where  $f_i$  is the fractional intensity contributed by species  $i$  ( $\sum f_i = 1$ ) with self-diffusion coefficient  $D_i$  and longitudinal and transverse relaxation times of  $T_{1i}$  and  $T_{2i}$ , respectively.

To extract diffusion coefficients from the experimental data, the resonance intensities  $I$  were plotted versus  $[(\gamma g \delta)^2 (\Delta - \delta/3)]$ , from which  $D$  values could be calculated either from equation (3) for single species, or from equation (4) for two species.

$$y = B + A \times \exp(-x \times D) \quad (3)$$

$$y = B + A_{uni} \times \exp(-x \times D_{uni}) + A_{mic} \times \exp(-x \times D_{mic}) \quad (4)$$

where  $D_{uni}$  and  $D_{mic}$  are the corresponding diffusion coefficients. The fractions of each independently diffusing species,  $f_{uni}$  and  $f_{mic}$  in the case of PFS-PI in high temperature decane solution, can be estimated from the combination of equations (5) and (6)

$$A_{uni}/A_{mic} = [f_{uni} \exp(-2\tau_2/T_{2uni}) \exp(-\tau_1/T_{1uni})] / [f_{mic} \exp(-2\tau_2/T_{2mic}) \exp(-\tau_1/T_{1mic})] \quad (5)$$

$$f_{uni} + f_{mic} = 1 \quad (6)$$

where  $A_{uni}$  and  $A_{mic}$  are obtained from exponential fitting of experimental data, and the relaxation times  $T_1$  and  $T_2$  for unimers and micelles should be determined at each temperature.

The details of the experimental setup are shown in Table 1 and 2, for measuring diffusion coefficients of solvent decane and sample PFS<sub>65</sub>-*b*-PI<sub>637</sub> (6 mg/mL), respectively. The diffusion coefficients of solvent decane at different temperatures were employed to calculate the solution viscosity at each temperature, so that the hydrodynamic radii of the PFS<sub>65</sub>-*b*-PI<sub>637</sub> micelles seeds could be calculated from measured  $D$  values using the Stokes-Einstein equation

$$R_h = k_B T / (6\pi\eta D) \quad (7)$$

**Table 1. Template for DOSY experiments of solvent decane <sup>a</sup> with DMSO-*d*<sub>6</sub>-insert**

NMR <sup>b</sup>	Dpfgdste
------------------	----------

Temperature (°C)	25	50	75	80	85	90	95	100
Lowest Gradient	1000	1000	1000	1000	1000	1000	1000	1000
Highest Gradient	4500	4000	3300	3100	3000	2900	2800	2700

- a. All experiments were run with a capillary insert containing DMSO-d<sub>6</sub> as deuterium lock.
- b. Using relaxation time 5 s, number of scans 4, diffusion gradient length 4.5 ms, diffusion delay 200 ms, grad stab delay 0.5, and 15 increments.

VT-DOSY spectra of PFS<sub>65</sub>-*b*-PI<sub>637</sub> micelle fragment solutions in decane were obtained at various temperatures ranging from 25 to 100 °C. Two sets of VT-DOSY measurements were carried out using micelle solutions with different sample histories. In the first set of experiments (denoted DOSY.01), only one micelle solution (6 mg/mL in decane) was used. This solution was heated to elevated temperatures stepwise from 25 to 100 °C, with DOSY measurements recorded at discrete temperature intervals. In the second set of experiments (DOSY.02), a series of identical samples were prepared. Here a sample was used for a DOSY measurement at only one temperature, so that results for experiments at different temperatures refer to separate samples.

**Table 2. Template for DOSY experiments of PFS<sub>65</sub>-*b*-PI<sub>637</sub> micelle fragments in decane <sup>a</sup>**

Pulse Sequence <sup>b</sup>	Dpfgdste							
Temperature (°C)	25	50	75	80	85	90	95	100
Diffusion delay Δ (ms)	900	650	450	200	250	200	150	50

- a. All experiments were run with a capillary insert containing DMSO-d<sub>6</sub> as deuterium lock.
- b. Using relaxation time 5 s, number of scans 32, gradient range 1000 – 28000, diffusion gradient length 4.5 ms, grad stab delay 0.5, and 15 increments.

## RESULTS AND DISCUSSIONS

### *Polymer Purification.*

The PFS<sub>65</sub>-*b*-PI<sub>637</sub> polymer used in this DOSY study was synthesized by anionic ring-opening polymerization and was originally reported<sup>30</sup> to have a composition of PFS<sub>53</sub>-*b*-PI<sub>637</sub>,

where the PI was found to have  $DP_n = 637$  and the block ratio was determined by comparing  $^1H$  NMR integration values of the PFS and PI signals for samples in a common good solvent, repeated here using benzene- $d_6$ , Figure 1a. By DOSY NMR (Figure 1b) of micelle fragment samples in decane, we found that the stimulated echo intensity attenuation as a function of the gradient strength fit much better to the two-exponential function (red solid line) than a single exponential (blue solid line). This was an indication of the presence of two species in the sample solution with different diffusion rates. The slow diffusing species, was characterized by  $D = 6.1 \times 10^{-8} \text{ cm}^2/\text{s}$  and its hydrodynamic radius ( $R_h$ ) was calculated to be 40 nm. The fast diffusing species, with  $D = 7.3 \times 10^{-7} \text{ cm}^2/\text{s}$  ( $R_h = 6 \text{ nm}$ ), was consistent with a small amount of  $PI_{637}$  homopolymer. It should be noted that for the experiments reported in ref 30, the presence of this homopolymer would not interfere with any of the self-assembly experiments reported.

This impurity was removed by fractional precipitation. By comparing the integration of signals of the cyclopentadiene rings in the PFS block in the  $^1H$  NMR spectrum to signals from the PI block, as shown in Figure 1c, we found that the purified polymer had the composition  $PFS_{65}\text{-}b\text{-}PI_{637}$ . In Figure 1d the DOSY NMR of the purified sample as micelle fragments in decane also showed that only one species was present, with  $R_h = 38 \text{ nm}$ . In Figure S2 we compare GPC traces in THF of the original “ $PFS_{53}\text{-}b\text{-}PI_{637}$ ” sample and the sample denoted  $PFS_{65}\text{-}b\text{-}PI_{637}$  after purification. Both peaks are monomodal, but after purification there was a decrease in  $\bar{M}$  from 1.07 to 1.04.

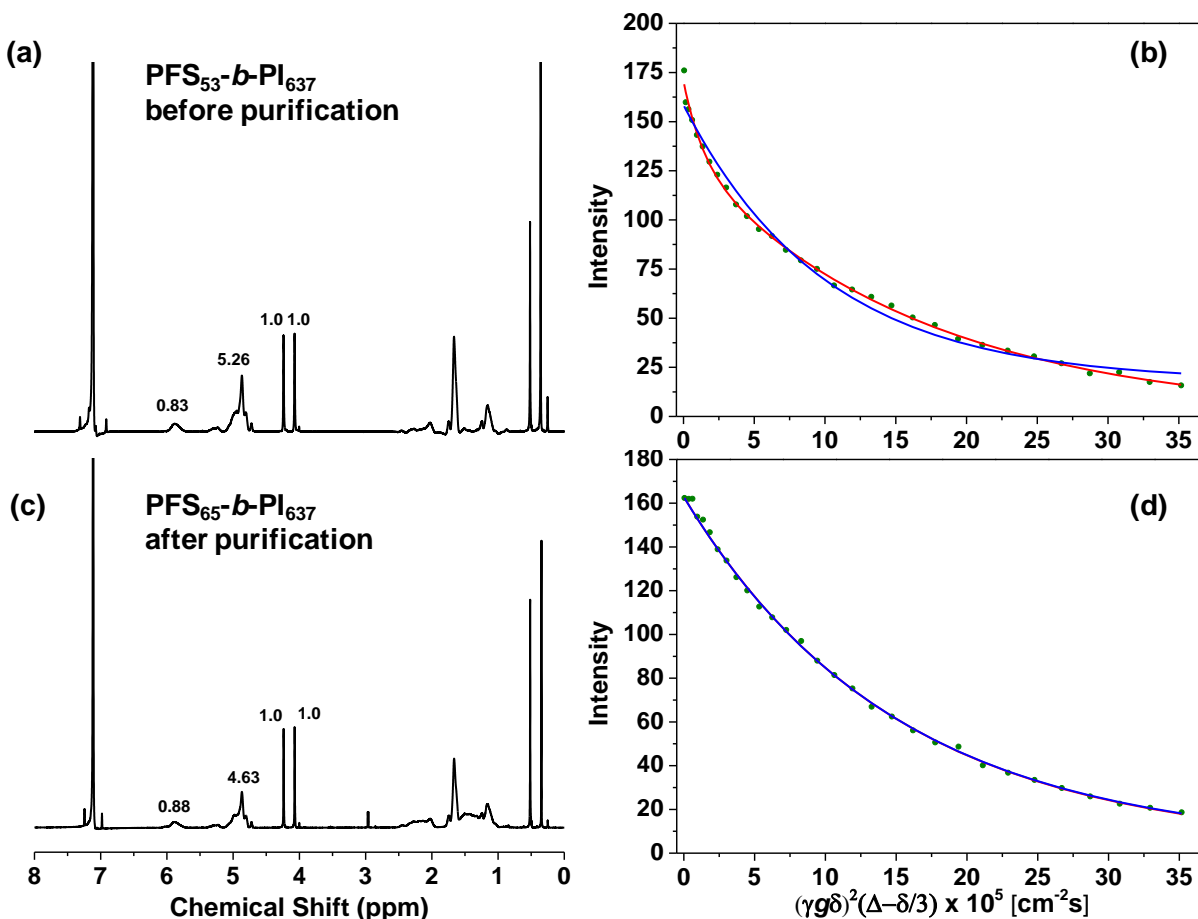


**Figure 1.**  $^1\text{H}$  NMR spectra of the original “ $\text{PFS}_{53}\text{-}b\text{-PI}_{637}$ ” sample in  $\text{C}_6\text{D}_6$  (a) before and (c) after purification to remove a small amount of  $\text{PI}_{637}$  homopolymer impurity. The calculated composition changed to  $\text{PFS}_{65}\text{-}b\text{-PI}_{637}$  after purification by fractional precipitation. Stimulated echo intensity attenuation  $I$  of the NMR signal at 4.4–5.1 ppm as a function of the gradient strength ( $G$ ) at 25 °C. The NMR signal is due to resonances of PI protons from micelle fragment samples in decane prepared from (b) “ $\text{PFS}_{53}\text{-}b\text{-PI}_{637}$ ” prior to purification and (b) from  $\text{PFS}_{65}\text{-}b\text{-PI}_{637}$  after purification to remove a  $\text{PI}_{637}$  homopolymer impurity. The spectra were run with  $\text{DMSO-d}_6$  in a capillary insert. In (d), the solid red line is the curve of best fit obtained using a two-exponential function, and the blue solid line is the curve of best fit obtained using a mono-exponential function.

### *Decane viscosities at different temperatures.*

In order to convert diffusion coefficients determined at different temperatures to hydrodynamic radii, we needed values of the viscosity of decane at these temperatures. These viscosity values are known for some temperatures, but in order to interpolate values over the entire range, we measured  $D_s$  values of neat decane over the entire temperature range.<sup>32</sup> At 25 °C, where the viscosity of decane is known, we calculated  $R_h = 0.19$  nm from the measured  $D_s$  value.<sup>33</sup> Since decane is a small organic molecule, we assumed that the magnitude of  $R_h$  would

not change significantly in this temperature range. Values of the measured  $D_s$  and corresponding calculated solvent viscosity values  $\eta$  are collected in Table S1. In Figure 2 the experimental viscosities are compared with the reported literature values<sup>34</sup> and show a good match.

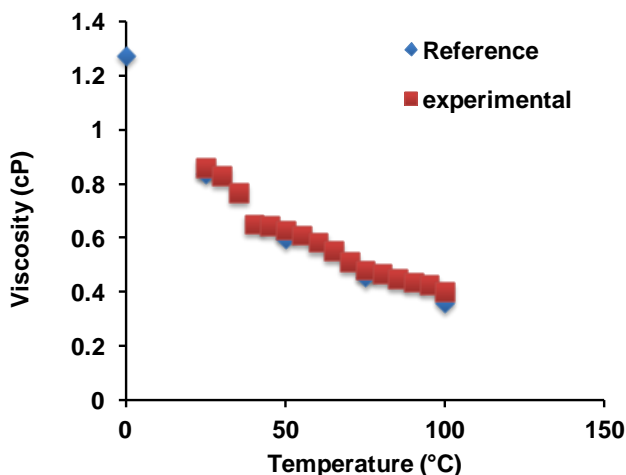


**Figure 2.** Comparison of experimental and literature values of the viscosities of decane at various temperatures from 0 to 100 °C.

### *Diffusive Motion for polymer samples at Room Temperature.*

Sample preparation began with the formation of long fiber-like micelles using the purified sample of PFS<sub>65</sub>-*b*-PI<sub>637</sub>. This polymer in decane ( $c = 6.0$  mg/mL) was heated at 100 °C for 30 min and then allowed to cool slowly to room temperature. After aging at room temperature for a day the sample was subjected to mild sonication to produce micelles fragments which we sometimes refer to as seeds. These micelle fragments are relatively uniform in size as shown in the TEM image in Figure 3, characterized by  $L_n = 39$  nm,  $L_w = 44$  nm.

As mentioned above, the  $^1\text{H}$  NMR of PFS<sub>65</sub>-*b*-PI<sub>637</sub> in benzene- $d_6$  (Figure 1c), a common good solvent showed peaks for both the PI and PFS components. In contrast, at 25 °C, the  $^1\text{H}$  NMR of PFS<sub>65</sub>-*b*-PI<sub>637</sub> micelle fragments in decane (Figure 3c) gave peaks 4.6 and 5.7 ppm associated with the PI corona, but no signals from PFS. We know that under these conditions, all of the PFS chains are confined to the micelle core. Not surprisingly, the mobility of these chains is too restricted to contribute to the high resolution NMR spectrum in Figure 3c.

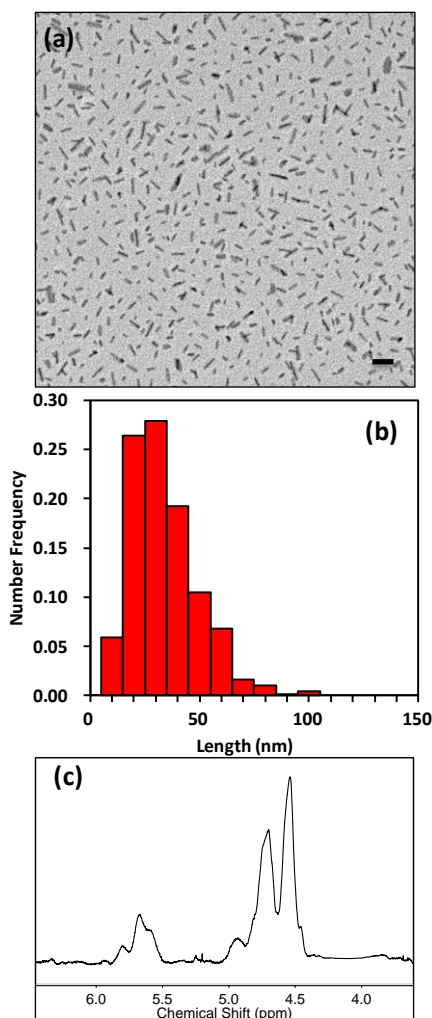


**Figure 3.** (a) TEM image (scale bar = 100 nm) and (b) histogram of the length distribution of PFS<sub>65</sub>-PI<sub>637</sub> micelle fragments prepared in decane. From the histogram, we calculate  $L_n = 39$  nm,  $L_w = 44$  nm. (c) Proton NMR spectrum of PFS<sub>65</sub>-*b*-PI<sub>637</sub> micelle seeds in decane (6 mg/mL) at 25 °C. The small shift in the peak positions of the PI protons here compared to those in Figure 1 is due to the difference in solvent.

The diffusive motion of PFS<sub>65</sub>-*b*-PI<sub>637</sub> unimers in benzene-*d*<sub>6</sub> and PFS<sub>65</sub>-*b*-PI<sub>637</sub> micelle fragments in decane was studied by DOSY NMR. A typical PFG-SE <sup>1</sup>H NMR spectral data set showing the intensity decay for the sample in benzene-*d*<sub>6</sub> is shown in Figure 4. From bottom to top, the intensities of the peaks decay with increasing magnetic field gradient strength (*g*). The choices of the lowest and highest gradients were determined such that the peak intensity decayed to 10% of its original value in the last increment. A total number of 31 increments were used in each DOSY experiment to ensure that there would be enough valid data points to calculate the diffusion coefficient. For this purified PFS<sub>65</sub>-*b*-PI<sub>637</sub> sample, the stimulated echo intensity decays fit well to a single exponential term (eq 1) for the PI signal intensities measured at 4.5-5.4 ppm

and for the PFS signal intensities measured at 4.1-4.3 ppm (Figure 5). Data analysis of the PI signal led to a  $D_s = 5.3 \times 10^{-7} \text{ cm}^2/\text{s}$ , whereas analysis of the PFS signal gave  $D_s = 4.9 \times 10^{-7} \text{ cm}^2/\text{s}$ . As the two blocks are covalently connected, block copolymer must diffuse as a single entity; thus the 7% difference between the two fitted  $D_s$  values is an indication of the accuracy of the measurement. From the Stokes-Einstein equation, the average hydrodynamic radius of the unimer was calculated to be 7.1 nm.

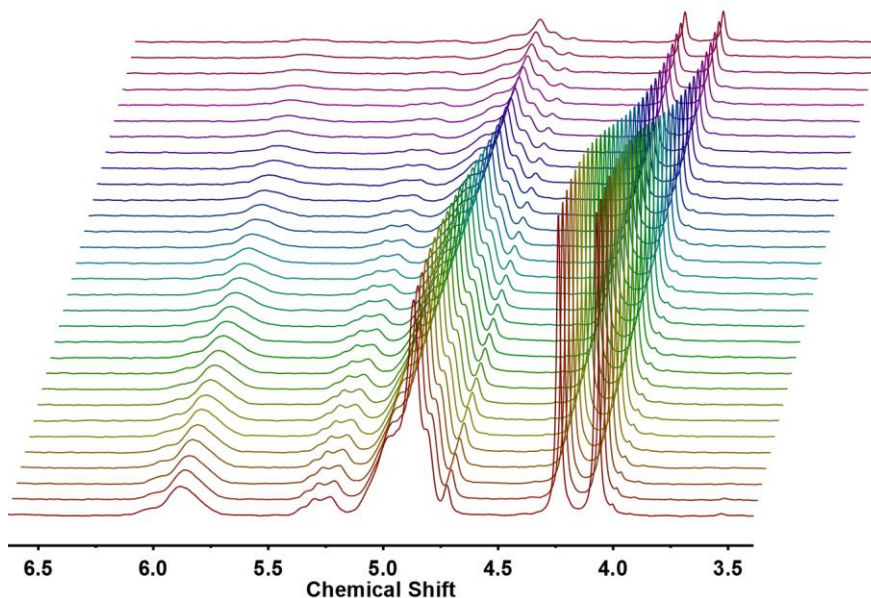


**Figure 4.** Typical PFG  $^1\text{H}$  NMR spectra for  $\text{PFS}_{65}\text{-}b\text{-PI}_{637}$  polymers (6 mg/mL) in benzene- $\text{d}_6$  at 25 °C as a function of magnetic gradient amplitude ( $g$ ) from low (bottom) to high (top).

DOSY NMR measurements at 25 °C were used to examine the diffusive motion of the  $\text{PFS}_{65}\text{-}b\text{-PI}_{637}$  micelle seed sample. As shown in Figure 1d, the intensity decay also fit well to a single exponential term, characterized by  $D_s = 6.7 \times 10^{-8} \text{ cm}^2/\text{s}$ , corresponding to  $R_h = 38 \text{ nm}$ , which is very close to the number average length of these micelle fragments (39 nm) determined by TEM. These DOSY NMR experiments show that the  $\text{PFS}_{65}\text{-}b\text{-PI}_{637}$  unimers and the micelle seeds formed by this block copolymer have very different diffusion rate that can be readily distinguished. This finding is important as it suggests that DOSY could be a promising tool to study the micelle dissolution at elevated temperatures, where both unimers and micelles will be present at the same time.

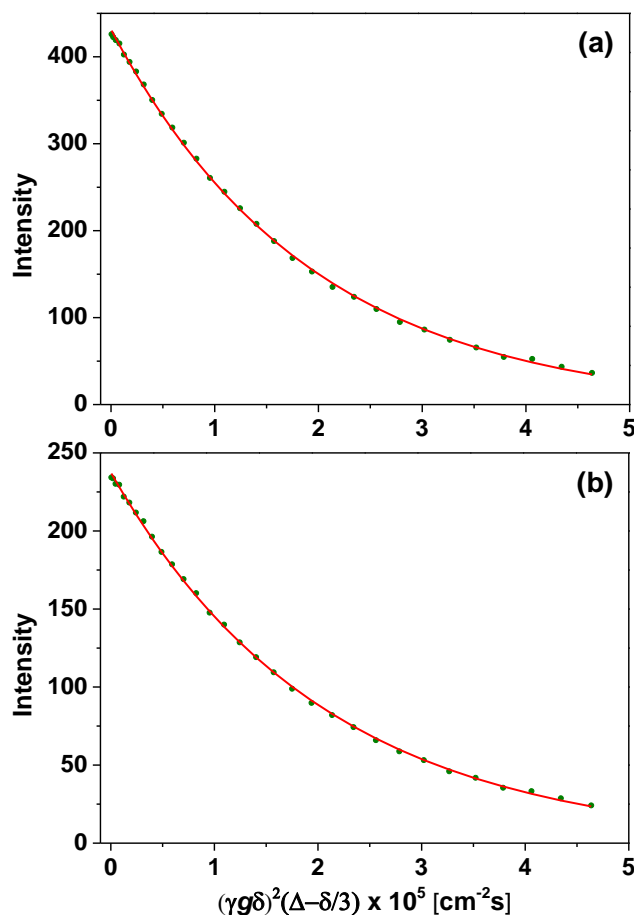


**Figure 5.** Stimulated echo intensity attenuation  $I$  of the PFS<sub>65</sub>- $b$ -PI<sub>637</sub> NMR signal at 4.5-5.4 ppm (PI, left) and 4.1-4.3 ppm (PFS, right) in C<sub>6</sub>D<sub>6</sub> as a function of the gradient strength  $g$ . Diffusion coefficients of  $5.3 \times 10^{-7} \text{ cm}^2/\text{s}$  and  $4.9 \times 10^{-7} \text{ cm}^2/\text{s}$  were calculated from PI and PFS signals, respectively.

### ***Monitoring Micelles Dissolution at Elevated Temperatures.***

**Variable temperature NMR measurements.** In the first set of experiments, a single solution of PFS<sub>65</sub>- $b$ -PI<sub>637</sub> micelle fragments ( $L_n = 39 \text{ nm}$ ,  $L_w = 44 \text{ nm}$ ) in decane (6 mg/mL) was heated stepwise through a series of temperatures. The  $^1\text{H}$  NMR spectrum was recorded at two different time point at each temperature. One spectrum was taken as soon as the instrument indicated that that temperature had been reached. A second spectrum was take 15 min later. Then the temperature of the sample was increased to the next step. Spectra were taken with a pulse sequence that supressed signals from the solvent decane.<sup>35</sup> [ref added] A series of spectra, covering the range of 3.5 to 6.5 ppm for temperatures between 50 °C and 100 °C are presented in Figure 6a. The peaks due to PI protons do not change in shape significantly over this range of



temperatures. The spectra were normalized so that the integration of PI peaks from 4.4 to 5.1 ppm remain constant. Signals from PFS block started to appear at 70 °C and the intensity became stronger with increasing temperature. At 100 °C, the ratio of intensities for the PFS peaks to the PI peaks was essentially the same as detected in the room temperature spectrum in benzene- $d_6$ . This result indicates that all of the BCP in the micelles had dissolved at this temperature.

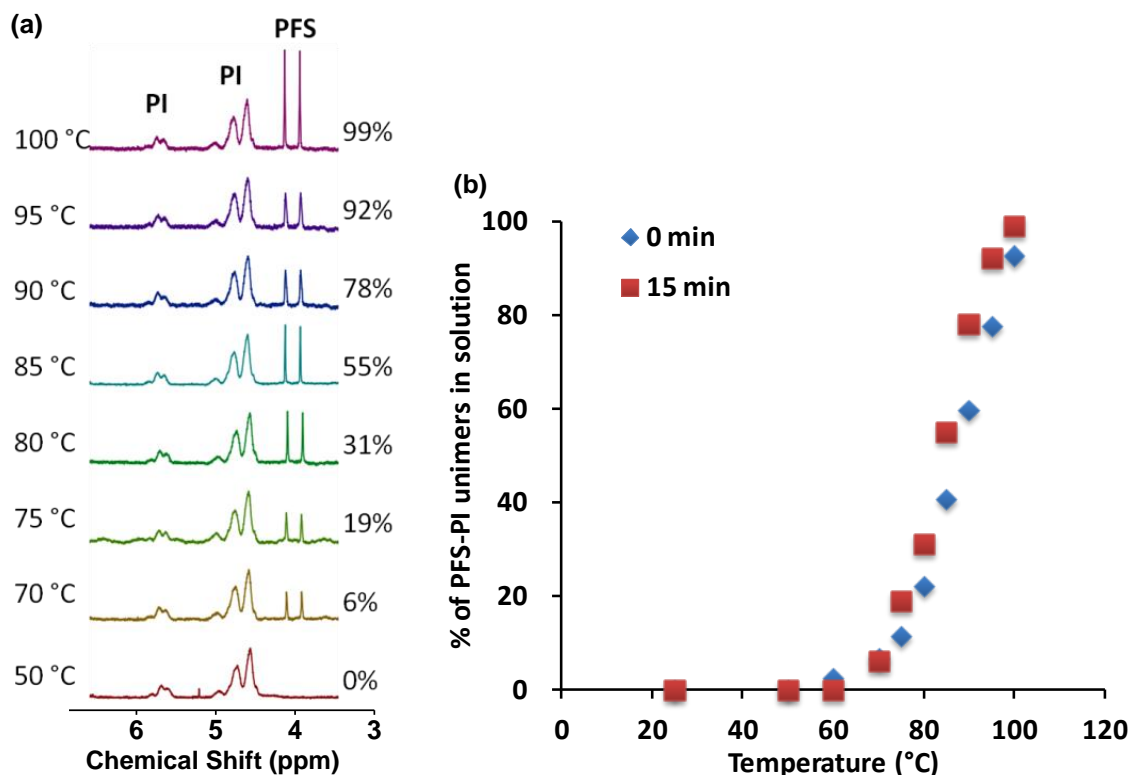


**Figure 6.** (a)  $^1\text{H}$  NMR spectra of  $\text{PFS}_{65}\text{-}b\text{-PI}_{637}$  micelle fragments in decane at various temperatures from 50 to 100 °C. These spectra were taken from samples immediately after they reached the desired temperature. (b) The percentage of  $\text{PFS}_{65}\text{-}b\text{-PI}_{637}$  present as dissolved unimers at each temperature. This percentage was calculated from the ratio of PFS to PI signal integrations, assuming that the intensity of the PI signal remains constant at each temperature. In order to test whether kinetic factors affected the fraction of BCP that dissolved at each temperature, NMR spectra were measured at 0 min and 15 min after the probe reached the desired temperature.

In Figure 6b we plot the fraction (percentage) of the BCP that had dissolved at each temperature. This fraction was calculated by comparing the integrated intensities of the two PFS peaks at ca. 4 ppm to the integrated intensities of the PI peaks at 4.4 to 5.1 ppm. This analysis assumes that the signal from the mobile PI corona chains remains constant at all temperatures. In order to test whether there was a kinetic component to the dissolution of BCP molecules from the micelle fragments, we carried out a second NMR measurement at each temperature. This measurement was made 15 min after the initial measurement. Figure 6b shows that, at each

temperature, there was a small increase in the fraction of polymer that had dissolved in the samples aged for this additional time. No further changes in the spectra were found for samples aged longer than 15 min at any temperature.

The results in Figure 6 are entirely consistent with the self-seeding behavior of PFS-*b*-PI micelle fragments in decane. In those experiments, heating a micelle solution in this temperature range, led, upon cooling, to a smaller number of micelles uniform in length. The number and length of the micelles formed remained constant for samples annealed for times between 30 min and 24 hr before letting them cool to room temperature. The explanation proposed for this behavior is that the PFS domains of lowest crystallinity were the first to dissolve as the sample was heated, and that at increasing temperature, domains of higher crystallinity dissolved, until only the most crystalline seed fragments remained intact. As we see in Figure 6, the fraction of polymer that dissolved increased sensitively with increasing temperature. Since the melting or dissolution temperature of a semicrystalline polymer is related to its degree of crystallinity, we can understand that heating a solution of micelle fragments for more than 15 min at a given temperature leads to the equilibrium solubility of the surviving micelle fragments.

**DOSY NMR measurements.** The experiments described in the previous section allowed us to quantify the fraction of polymer in the core-crystalline micelle fragments that dissolved when their solutions were heated to typical self-seeding temperatures. Here we explore whether DOSY measurements at elevated temperatures can complement these experiments by determining the corresponding diffusion coefficients of the mobile species in solution. Initial high temperature experiments, carried out with a traditional PFG-SE pulse sequence, gave results that appeared to be distorted because of convection in the sample tube. Therefore we turned to the Pulsed Field Gradient Double STimulated Echo (Dpfgdste) pulse sequence developed by Jerschow and Muller<sup>25</sup> to compensate for these complications.

DOSY experiments at room temperature showed that the characteristic  $R_h$  of our micelle fragment sample was 38 nm. DOSY measurements should be sensitive to changes in micelle size as polymer from these fragments dissolved.

In the first set of experiments (DOSY.01), a single sample of PFS<sub>65</sub>-*b*-PI<sub>637</sub> micelle fragments (6.0 mg/mL in decane) was heated stepwise to various temperatures from 25 to 100 °C. Data acquisition was relatively slow, and each DOSY measurement at each temperature required 2 hours to complete. Intensity decay profiles were measured for both the PI signal at 4.4-5.1 ppm

and the PFS at 3.8-4.2 ppm. These experimental data were then fitted using a mono-exponential function eq (1). When the quality of this fit was poor, suggesting the presence of two independent diffusing species (unimer and micelle), the data were then fitted to a sum of two exponential terms, eq (2). In Table 4, we present the values of the diffusion coefficients  $D_s$  determined in this way, along with  $R_h$  values calculated using the appropriate viscosity of decane at that temperature.

At 25 °C, we found only a single (slow) diffusing species, the intact micelle fragment, with  $R_h = 38$  nm. At the two highest temperatures (95, 100 °C), we found only a single (fast) diffusing species with  $R_h \approx 5.5$  nm. We found similar values of  $D_s$  and  $R_h$  from measurements of both the PI signals and the PFS signals in the NMR. Based on measurements at 25 °C in benzene- $d_6$ , where we found  $R_h \approx 7$  nm, we can assign the fast diffusing species to the PFS<sub>65</sub>-*b*-PI<sub>637</sub> unimer. At 80, and 85 °C, the decay of the PFS signal followed a single exponential profile, with we associate with unimer. At 70 and 75 °C, the PFS signal was too weak to obtain a meaningful fit. In contrast, fitting the PI decays at 70, 75, 80, and 85 °C required two exponential terms, indicating that micelle fragments and unimers were both present. The fast decays determined from both the PFS and PI signals were consistent with  $R_h \approx 5 - 7$  nm. The slow decays gave a value of  $R_h = 45$  nm at 70 °C, decreasing to ca. 36 nm at 80 and 85 °C. Given that we obtained these values from a fit to two exponential terms, of data covering only one decade of intensity decay, this difference may not be significant.

One of the problems with the data collected for the DOSY.01 experiments is that the samples were annealed at successively increasing temperatures over many hours. It is well known that samples of semi-crystalline polymers remodel when heated but annealed at temperatures below the melting point. For typical platelet homopolymer crystals, the platelets become thicker and the degree of crystallinity increases.<sup>36, 37</sup> [ref added] Less is known about core-crystalline micelles, but we recently examined one sample of PFS<sub>65</sub>-*b*-PI<sub>637</sub> micelle fragments annealed in decane at 75 °C.<sup>38</sup> Here we found an increase in the number of BCP molecules per nm of micelle length, and TEM tomography measurements showed that the micelle core became wider and more rectangular.

**Table 4. DOSY.01 Experimental diffusion coefficients and calculated  $R_h$  values of PFS<sub>65</sub>-*b*-PI<sub>637</sub> unimer and micelle fragments in decane at various temperatures <sup>a</sup>**

DOSY.01 <sup>b</sup>	$10^8 \times D_s$ (cm <sup>2</sup> /s)		$R_h$ (nm)		R <sup>2</sup> values of the fits	
T °C	PI signal	PFS signal	PI signal	PFS signal	PI signal	PFS signal
25	6.7	--	38	--	0.9991	--
70	11 72	--	45 6.9	--	0.9998	--
75	12 86	--	43 6.1	--	0.9998	--
80	15 97	130	36 5.7	4.3	0.9998	0.9673
85	16 93	87	37 6.3	6.7	0.9997	0.9958
90	74	89	8.1	6.8	0.9982	0.9953
95	120	120	5.5	5.3	0.9992	0.9975
100	120	130	5.6	5.5	0.9997	0.9979

a. A capillary tube insert containing DMSO-d<sub>6</sub> was used as a deuterium lock

b. In DOSY.01 experiments, a single sample of micelle fragments in decane was examined step-wise at each increasing temperature. The measurement at each temperature took ca. 2 h.

In order to minimize sample history effects on our PFS<sub>65</sub>-*b*-PI<sub>637</sub> micelle fragment sample, we carried out a second set of DOSY experiments (DOSY.02). Here we prepared multiple identical samples, each at 6 mg/mL. We used one sample for each temperature. Each sample was held at the measurement temperature for about 2 h, but the extent of annealing for the samples measured at the highest temperatures was reduced. The results are summarized in Table 5. The PFS signal could be detected starting at 75 °C, and these intensity decays gave good fits to a single exponential function. Values of  $R_h$  were in the range of 5.1 – 5.9 nm at all temperatures, indicating that the unimer does not change its dimensions significantly in this temperature range. At 90, 95, and 100 °C, the PI signal decay also fit well to one exponential. Calculated values of  $R_h$  were close to those determined from the PFS signal. While the VT-NMR experiments suggested that not all micelle fragments dissolved below 100 °C, its contribution to the PI signal decay in the DOSY experiment was not significant.

At 79, 75, 80 and 85 °C, the fits to the PI decay required two exponential terms. The fast decay gave  $R_h$  values somewhat smaller than those found from the PFS decays. These differences are likely a consequence of fitting three independent parameters (eq 2) instead of one (eq 1). Another interesting feature of these experiments is that the size of the surviving micelle fragments appears to decrease, from  $R_h = 39$  nm at 70 °C to 21 nm at 85 °C. We plot values of all of the  $R_h$  values obtained through DOSY measurements in Figure 7. This plot emphasizes that the size of the unimer does not change over the range of temperatures examined. In contrast, the two sets of DOSY experiments gave somewhat different results for the size of the surviving seed at temperatures between 70 and 85 °C. The first set of experiments suggests a small decrease in  $R_h$  from 45 nm to 36 nm with increasing temperature. The second set of experiments (DOSY.02) suggested a more striking decrease in size, from 40 nm to 24 nm over this temperature range.

**Table 5. DOSY.02 Experimental diffusion coefficients and calculated  $R_h$  values of PFS<sub>65</sub>-*b*-PI<sub>637</sub> unimer and micelle fragments in decane at various temperatures <sup>a</sup>.**

DOSY.02 <sup>b</sup>	$10^8 \times D_s$ (cm <sup>2</sup> /s)		$R_h$ (nm)		$R^2$ values of the fits	
T °C	PI signal	PFS signal	PI signal	PFS signal	PI signal	PFS signal
25	6.7	--	38	--	0.9991	--
70	13 110	-	39 4.5	--	0.9994	--
75	17 120	100	32 4.5	5.1	0.9998	0.9876
80	21 120	94	26 4.5	5.9	0.9999	0.9982
85	27 110	99	21 5.2	5.9	0.9996	0.9986
90	99	110	6.1	5.6	0.9994	0.9970
95	110	110	5.5	5.8	0.9987	0.9975
100	120	120	5.8	5.9	0.9999	0.9997

a. A capillary tube insert containing DMSO-d<sub>6</sub> was used as a deuterium lock

b. In DOSY.02 experiments, separate samples of micelle fragments in decane were prepared for each temperature. The samples were heated rapidly to the measurement temperature. Then measurement at each temperature took ca. 2 h.

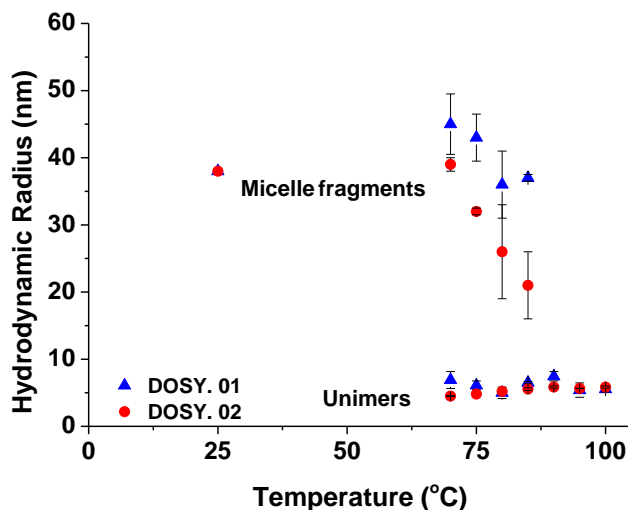


**Figure 7.** Hydrodynamic radii of all the species detected by DOSY NMR at temperatures from 25 to 100 °C in decane.

Lastly, we examined whether we could fit the two-component DOSY data to eq 5 as an independent measurement of the fraction of material present as micelle fragments and as unimer. This turned out to not to be possible without further strong assumptions about the data, since this analysis requires experimental values of  $T_1$  and  $T_2$  of each species at each temperature. Further comments about this analysis and the assumptions that need to be made are provided in SI.

## SUMMARY

We used variable temperature (VT)  $^1\text{H}$  NMR to examine the behavior of short core-crystalline micelle fragments of  $\text{PFS}_{65}\text{-}b\text{-PI}_{637}$  BCP micelles in decane subjected to self-seeding conditions. The self-seeding phenomenon is normally explained in terms of a distribution of crystallites with different degrees of crystal perfection. As a sample is heated, the least crystalline domains dissolve and the more highly crystalline domains persist. Upon cooling, all

of the dissolved polymer grows onto the surviving crystallites that serve as nuclei for crystal growth. Studies of self-seeding suggest that the fraction of surviving seed crystallites at a given temperature remains constant independent of the annealing time at that temperature.

VT NMR allowed us to monitor the fraction of BCP that dissolved as a function of temperature. We examined a sample of micelle fragments of PFS<sub>65</sub>-*b*-PI<sub>637</sub> characterized by  $L_n = 39$  nm,  $L_w/L_n = 1.13$ . Our experiments took advantage of the high mobility of the PI corona chains in the micelle, that give a <sup>1</sup>H NMR signal that was independent of whether the PI was present as corona chains in the micelles or as discrete molecules (unimer). In contrast, the PFS component could be detected only for the dissolved unimer. In this way, we found that all of the BCP molecules were incorporated into the micelles at temperatures up to and including 50 °C. Both PFS and PI resonances could be detected between 70 and 100 °C, and at 100 °C, the integration ratio of the PFS-to-PI peaks was essentially the same as for a solution of the BCP in benzene-d<sub>6</sub>, a common good solvent. Thus we infer that all of the polymer had dissolved at 100 °C. At intermediate temperatures in decane, the extent of dissolution remained constant over time. This result confirms an idea inferred from self-seeding experiments.

We also examine pulsed-gradient spin-echo (DOSY NMR) experiments at these temperatures with the goal of measuring self-diffusion coefficients ( $D_s$ ) for the micelle fragments and unimers. We then used these  $D_s$  values in conjunction with the Stokes-Einstein equation to calculate hydrodynamic radii ( $R_h$ ) for these species. At temperatures between 80 and 100 °C, the intensity decay signals due to PFS were well-fit to a single exponential, giving  $R_h$  values in the range of 5 to 6 nm, consistent with unimer diffusion. At 25 °C, the PI signal was also characterized by a single exponential term with  $R_h = 38$  nm, characteristic of the micelle fragments. At 90, 95, and 100 °C, the decay was also well-fitted to an exponential profile, with

$R_h \approx 6$  nm, corresponding to unimer. At intermediate temperatures, the DOSY signal decay for PI could be fitted to a sum of two exponential terms, consistent with a fast diffusing species with  $R_h \approx 5$  to 6 nm and a slow diffusing species with an  $R_h$  value that decreased with increasing temperature. The most interesting aspect of the DOSY results is that the size of the micelle fragments at elevated temperatures (80, 85 °C) was sensitive to sample history, with smaller fragments (26, 21 nm) obtained for samples heated quickly to the measurement temperature. Samples subjected to prolonged annealing at lower temperatures showed much smaller reduction in  $R_h$  (36, 37 nm) when heated to 80 or 85 °C.

DOSY NMR is a very interesting method to investigate the dissolution of core-crystalline micelles upon heating and the evolution of micelle size. Our experiments provide useful insights into the strengths and limitations of this methodology.

## ASSOCIATED CONTENT

### Supporting Information Available:

Additional results and discussion, pulse sequence used for the DOSY measurements, GPC of block copolymers before and after purification. This material is available free of charge via the Internet at <http://pubs.acs.org>.

## AUTHOR INFORMATION

### Corresponding Author

\* E-mail: [mwinnik@chem.utoronto.ca](mailto:mwinnik@chem.utoronto.ca) (M.A.W.)

### Notes

The authors declare no competing financial interest.

## ACKNOWLEDGEMENTS

The Toronto authors thank NSERC Canada for their support of this research.



## REFERENCES

1. Mai, Y.; Eisenberg, A. Self-assembly of block copolymers. *Chem Soc Rev* **2012**, 41 (18), 5969-85.
2. T. Vilgis, A. H. Aggregation of coil-crystalline block copolymers: equilibrium crystallization. *Macromolecules* **1991**, 24 (8), 2090-2095.
3. Qian, J.; Zhang, M.; Manners, I.; Winnik, M. A. Nanofiber micelles from the self-assembly of block copolymers. *Trends Biotechnol* **2010**, 28 (2), 84-92.
4. Dean, J. M.; Verghese, N. E.; Pham, H. Q.; Bates, F. S. Nanostructure Toughened Epoxy Resins. *Macromolecules* **2003**, 36 (25), 9267-9270.
5. Dalhaimer, P.; Engler, A. J.; Parthasarathy, R.; Discher, D. E. Targeted worm micelles. *Biomacromolecules* **2004**, 5 (5), 1714-9.
6. Cao, L.; Manners, I.; Winnik, M. A. Influence of the Interplay of Crystallization and Chain Stretching on Micellar Morphologies: Solution Self-Assembly of Coil-Crystalline Poly(isoprene-block-ferrocenylsilane). *Macromolecules* **2002**, 35 (22), 8258-8260.
7. Jason A. Massey, K. T., Lan Cao, Yahya Rharbi, Jose Ruez, Mitchell A. Winnik, and, and Ian Manners. Self-Assembly of Organometallic Block Copolymers: The Role of Crystallinity of the Core-Forming Polyferrocene Block in the Micellar Morphologies Formed by Poly(ferrocenylsilane-b-dimethylsiloxane) in n-Alkane Solvents. *J Am Chem Soc* **2000**, 122 (47), 11577-11584.
8. Nichole Fairley, B. H., and Christine Allen. Morphological Control of Poly(ethylene glycol)-block-poly( $\epsilon$ -caprolactone) Copolymer Aggregates in Aqueous Solution. *Biomacromolecules* **2008**, 9 (9), 2283-2291.
9. Zi-Xiu Du; Jun-Ting Xu; and, a. Z.-Q. F. Micellar Morphologies of Poly( $\epsilon$ -caprolactone)-b-poly(ethylene oxide) Block Copolymers in Water with a Crystalline Core. *Macromolecules* **2007**, 40 (21), 7633-7637.
10. Fujiwara, T.; Miyamoto, M.; Kimura, Y.; Iwata, T.; Doi, Y. Self-Organization of Diblock and Triblock Copolymers of Poly(l-lactide) and Poly(oxyethylene) into Nanostructured Bands and Their Network System. Proposition of a Doubly Twisted Chain Conformation of Poly(l-lactide). *Macromolecules* **2001**, 34 (12), 4043-4050.

11. Zhang, J.; Wang, L. Q.; Wang, H.; Tu, K. Micellization phenomena of amphiphilic block copolymers based on methoxy poly(ethylene glycol) and either crystalline or amorphous poly(caprolactone-b-lactide). *Biomacromolecules* **2006**, 7 (9), 2492-500.
12. Schmalz, H.; Schmelz, J.; Drechsler, M.; Yuan, J.; Walther, A.; Schweimer, K.; Mihut, A. M. Thermo-Reversible Formation of Wormlike Micelles with a Microphase-Separated Corona from a Semicrystalline Triblock Terpolymer. *Macromolecules* **2008**, 41 (9), 3235-3242.
13. Lazzari, M.; Scalarone, D.; Hoppe, C. E.; Vazquez-Vazquez, C.; Lòpez-Quintela, M. A. Tunable Polyacrylonitrile-Based Micellar Aggregates as a Potential Tool for the Fabrication of Carbon Nanofibers. *Chemistry of Materials* **2007**, 19 (24), 5818-5820.
14. Lee, E.; Hammer, B.; Kim, J. K.; Page, Z.; Emrick, T.; Hayward, R. C. Hierarchical helical assembly of conjugated poly(3-hexylthiophene)-block-poly(3-triethylene glycol thiophene) diblock copolymers. *J Am Chem Soc* **2011**, 133 (27), 10390-3.
15. Qian, J.; Li, X.; Lunn, D. J.; Gwyther, J.; Hudson, Z. M.; Kynaston, E.; Rupar, P. A.; Winnik, M. A.; Manners, I. Uniform, high aspect ratio fiber-like micelles and block co-micelles with a crystalline pi-conjugated polythiophene core by self-seeding. *J Am Chem Soc* **2014**, 136 (11), 4121-4.
16. Kynaston, E. L.; Gould, O. E. C.; Gwyther, J.; Whittell, G. R.; Winnik, M. A.; Manners, I. Fiber-Like Micelles from the Crystallization-Driven Self-Assembly of Poly(3-heptylselenophene)-block-Polystyrene. *Macromolecular Chemistry and Physics* **2015**, 216 (6), 685-695.
17. Wang, X.; Guerin, G.; Wang, H.; Wang, Y.; Manners, I.; Winnik, M. A. Cylindrical block copolymer micelles and co-micelles of controlled length and architecture. *Science* **2007**, 317 (5838), 644-7.
18. Qian, J.; Guerin, G.; Lu, Y.; Cambridge, G.; Manners, I.; Winnik, M. A. Self-seeding in one dimension: an approach to control the length of fiberlike polyisoprene-polyferrocenylsilane block copolymer micelles. *Angew Chem Int Ed Engl* **2011**, 50 (7), 1622-5.
19. Qian, J.; Lu, Y.; Cambridge, G.; Guerin, G.; Manners, I.; Winnik, M. A. Polyferrocenylsilane Crystals in Nanoconfinement: Fragmentation, Dissolution, and Regrowth of Cylindrical Block Copolymer Micelles with a Crystalline Core. *Macromolecules* **2012**, 45 (20), 8363-8372.

20. Qian, J.; Lu, Y.; Chia, A.; Zhang, M.; Rupar, P. A.; Gunari, N.; Walker, G. C.; Cambridge, G.; He, F.; Guerin, G.; Manners, I.; Winnik, M. A. Self-seeding in one dimension: a route to uniform fiber-like nanostructures from block copolymers with a crystallizable core-forming block. *ACS Nano* **2013**, 7 (5), 3754-66.
21. D. J. Blundell; A. Keller; Kovacs, A. J. A NEW SELF-NUCLEATION PHENOMENON AND ITS APPLICATION TO THE GROWING OF POLYMER CRYSTALS FROM SOLUTION. *Journal of Polymer Science Part C: Polymer Letters* **1966**, 4 (7), 481-486.
22. Strobl, G. Crystallization and melting of bulk polymers: New observations, conclusions and a thermodynamic scheme. *Progress in Polymer Science* **2006**, 31 (4), 398-442.
23. Johnson, C. S. Diffusion ordered nuclear magnetic resonance spectroscopy: principles and applications. *Progress in Nuclear Magnetic Resonance Spectroscopy* **1999**, 34 (3-4), 203-256.
24. Morris, K. F.; Johnson, C. S. Resolution of Discrete and Continuous Molecular-Size Distributions by Means of Diffusion-Ordered 2d Nmr-Spectroscopy. *Journal of the American Chemical Society* **1993**, 115 (10), 4291-4299.
25. Jerschow, A.; Muller, N. Diffusion-separated nuclear magnetic resonance spectroscopy of polymer mixtures. *Macromolecules* **1998**, 31 (19), 6573-6578.
26. Viel, S.; Mazarin, M.; Giordanengo, R.; Phan, T. N.; Charles, L.; Caldarelli, S.; Bertin, D. Improved compositional analysis of block copolymers using diffusion ordered NMR spectroscopy. *Anal Chim Acta* **2009**, 654 (1), 45-8.
27. Cain, J. B.; Zhang, K.; Betts, D. E.; DeSimone, J. M.; Johnson, C. S. Diffusion of block copolymers in liquid CO<sub>2</sub>: Evidence of self-assembly from pulsed field gradient NMR. *Journal of the American Chemical Society* **1998**, 120 (36), 9390-9391.
28. Bakkour, Y.; Darcos, V.; Li, S.; Coudane, J. Diffusion ordered spectroscopy (DOSY) as a powerful tool for amphiphilic block copolymer characterization and for critical micelle concentration (CMC) determination. *Polymer Chemistry* **2012**, 3 (8).
29. Shen, L.; Soong, R.; Wang, M.; Lee, A.; Wu, C.; Scholes, G. D.; Macdonald, P. M.; Winnik, M. A. Pulsed field gradient NMR studies of polymer adsorption on colloidal CdSe quantum dots. *J Phys Chem B* **2008**, 112 (6), 1626-33.
30. Gilroy, J. B.; Rupar, P. A.; Whittell, G. R.; Chabanne, L.; Terrill, N. J.; Winnik, M. A.; Manners, I.; Richardson, R. M. Probing the structure of the crystalline core of field-aligned,

monodisperse, cylindrical polyisoprene-block-polyferrocenylsilane micelles in solution using synchrotron small- and wide-angle X-ray scattering. *J Am Chem Soc* **2011**, 133 (42), 17056-62.

31. Stejskal, E. O.; Tanner, J. E. Spin Diffusion Measurements: Spin Echoes in the Presence of a Time-Dependent Field Gradient. *The Journal of Chemical Physics* **1965**, 42 (1), 288-292.

32. Tofts, P. S.; Lloyd, D.; Clark, C. A.; Barker, G. J.; Parker, G. J.; McConville, P.; Baldock, C.; Pope, J. M. Test liquids for quantitative MRI measurements of self-diffusion coefficient in vivo. *Magn Reson Med* **2000**, 43 (3), 368-74.

33. Moore, J. W.; Wellek, R. M. Diffusion coefficients of n-heptane and n-decane in n-alkanes and n-alcohols at several temperatures. *Journal of Chemical & Engineering Data* **1974**, 19 (2), 136-140.

34. Haynes, W. M. CRC Handbook of Chemistry and Physics, 95th Edition. **2014**, 6-235.

35. Smallcombe, S. H.; Patt, S. L.; Keifer, P. A. WET solvent suppression and its applications to LC NMR and high-resolution NMR spectroscopy. *Journal of Magnetic Resonance Series A* **1995**, 117 (2), 295-303.

36. Rochette, C. N.; Rosenfeldt, S.; Henzler, K.; Polzer, F.; Ballauff, M.; Tong, Q.; Mecking, S.; Drechsler, M.; Narayanan, T.; Harnau, L. Annealing of Single Lamella Nanoparticles of Polyethylene. *Macromolecules* **2011**, 44 (12), 4845-4851.

37. Osichow, A.; Rabe, C.; Vogtt, K.; Narayanan, T.; Harnau, L.; Drechsler, M.; Ballauff, M.; Mecking, S. Ideal polyethylene nanocrystals. *J Am Chem Soc* **2013**, 135 (31), 11645-50.

38. Guerin, G.; Rupa, P.; Molev, G.; Mannes, I.; Jinnai, H.; Winnik, M. A. Lateral Growth of 1D Core-Crystalline Micelles upon Annealing in Solution. *Macromolecules* **2016**, 49 (18), 7004-7014.

## Table of Contents Graphic

